Digitally tunable physicochemical coding of material composition and topography in continuous microfibres

Article *in* Nature Materials · September 2011

DOI: 10.1038/nmat3108 · Source: PubMed

6 authors, including:

Gi Seok Jeong
Asan Medical Center
64 PUBLICATIONS **1,014** CITATIONS
SEE PROFILE

Kwang Ho Lee
Konkuk University
418 PUBLICATIONS **7,783** CITATIONS
SEE PROFILE

Ali Khademhosseini
University of California, Los Angeles
894 PUBLICATIONS **39,576** CITATIONS
SEE PROFILE

Sang-Hoon Lee
Korea University
710 PUBLICATIONS **11,243** CITATIONS
SEE PROFILE

nature materials

LETTERS

PUBLISHED ONLINE: 4 SEPTEMBER 2011 | DOI: 10.1038/NMAT3108

Digitally tunable physicochemical coding of material composition and topography in continuous microfibres

Edward Kang[1], Gi Seok Jeong[1], Yoon Young Choi[1], Kwang Ho Lee[1,2†], Ali Khademhosseini[3,4,5] and Sang-Hoon Lee[1*]

Heterotypic functional materials with compositional and topographical properties that vary spatiotemporally on the micro- or nanoscale are common in nature. However, fabricating such complex materials in the laboratory remains challenging. Here we describe a method to continuously create microfibres with tunable morphological, structural and chemical features using a microfluidic system consisting of a digital, programmable flow control that mimics the silk-spinning process of spiders. With this method we fabricated hydrogel microfibres coded with varying chemical composition and topography along the fibre, including gas micro-bubbles as well as nanoporous spindle-knots and joints that enabled directional water collection. We also explored the potential use of the coded microfibres for tissue engineering applications by creating multifunctional microfibres with a spatially controlled co-culture of encapsulated cells.

Micro- and nanoscale fibres have attracted substantial attention owing to their extensive applications[1–4]. Several methods have recently been developed to fabricate small fibres continuously, such as electrospinning and microfluidic spinning[5–8]. Most continuously generated fibres have been cylindrical in shape with a homogeneous chemical composition, and the creation of continuous microfibres with spatiotemporal variations in chemical composition and morphology has been a great challenge. The fibre-spinning mechanism of spiders may provide critical clues to addressing this challenge. The main features of this spinning process include its small scale, simplicity and tunability of the produced fibres. Microfluidic technology is one potential candidate that can achieve all of these features. Although microfluidic chips have been used extensively for fabricating particles with controlled shapes[9–14], the continuous production of fibres has presented a considerable challenge. Previous work by our group and others has demonstrated the feasibility of using microfluidics to engineer continuous fibres[8,15,16]. Recently, we reported the simultaneous production of multiple fibres, each of differing composition, using coaxial polydimethylsiloxane (PDMS) microfluidic channels[17]. Although these systems have broken several barriers of conventional methods, it has not been possible to generate fibres with complex morphologies and tunable composition to the same extent as those present in nature.

Here, we propose a spinning method that uses a microfluidic chip combined with a digital fluid controller. By introducing active functional modulations, such as by switching the flow through the use of a digital control scheme, we produced microfibres along which diverse chemical compositions, structures, gas bubbles, live cells and morphologies could be spatiotemporally coded. The coding resolution across the fibre was a few micrometres and could be regulated along the fibre to a few hundred micrometres. To our knowledge, such fibres have not previously been fabricated. Furthermore, an application of these fibres for tissue engineering was demonstrated by fabricating cell-laden microfibres with spatially regulated patterned cellular co-cultures. Similar to nature, in which functional materials are generated by combining diverse compositions of existing matter spatiotemporally, the proposed process may enable the creation of new materials by physicochemical modulation of existing materials on the microscale.

Insight from the spinning apparatus of spiders may be used to create a biomimetic approach to generate fibres. A spider produces fibres by mixing fluids from glands in its abdomen and spinning the resulting mixture (Fig. 1a). At the end of its spinning duct, a valve acts as a clamp to grip the thread or as a ratchet to restart spinning after internal rupture[18]. Fluids from different glands lead to the spinneret so that silk blends with specific properties, required for a particular function, can be produced[19]. We used a microfluidic process comprising a number of individually controllable inlets to generate a spinning process that mimics the spinning process of spiders. Figure 1b,c shows a schematic and an image of a microfluidic chip designed to produce microfibres with spatially organized morphologies and compositions. On this fluidic platform, the sample fluid volume of each channel is tightly controlled by a computer-controlled pneumatic valve (see Methods and Supplementary Fig. S1 for details). We used a thin PDMS membrane ($\approx$10 μm) and through a replication process we constructed hybrid channels (a combination of rectangular and cylindrical channels) on a single device[17]. Integrating small pneumatic valves into the hybrid channels was a critical technical challenge, which was addressed by using the parabolic membrane naturally generated by the surface tension

[1]Department of Biomedical Engineering, College of Health Science, Korea University, Jeongneung-dong, Seongbuk-gu, Seoul 136-703, Republic of Korea, [2]Department of Mechanical Engineering, Massachusetts Institute of Technology, 77 Massachusetts Avenue, Cambridge, Massachusetts 02139, USA, [3]Center for Biomedical Engineering, Department of Medicine, Brigham and Women's Hospital, Harvard Medical School, 65 Landsdowne Street, Cambridge, Massachusetts 02139, USA, [4]Harvard-MIT Division of Health Sciences and Technology, Massachusetts Institute of Technology, Cambridge, Massachusetts 02139, USA, [5]Wyss Institute for Biologically Inspired Engineering, Harvard University, Boston, Massachusetts 02115, USA. †Present address: Department of Advanced Materials Science and Engineering, Kangwon National University, Hyoja 2-dong, Chuncheon-si, Gangwon-do, 200-701, Republic of Korea. *e-mail: dbiomed@korea.ac.kr.

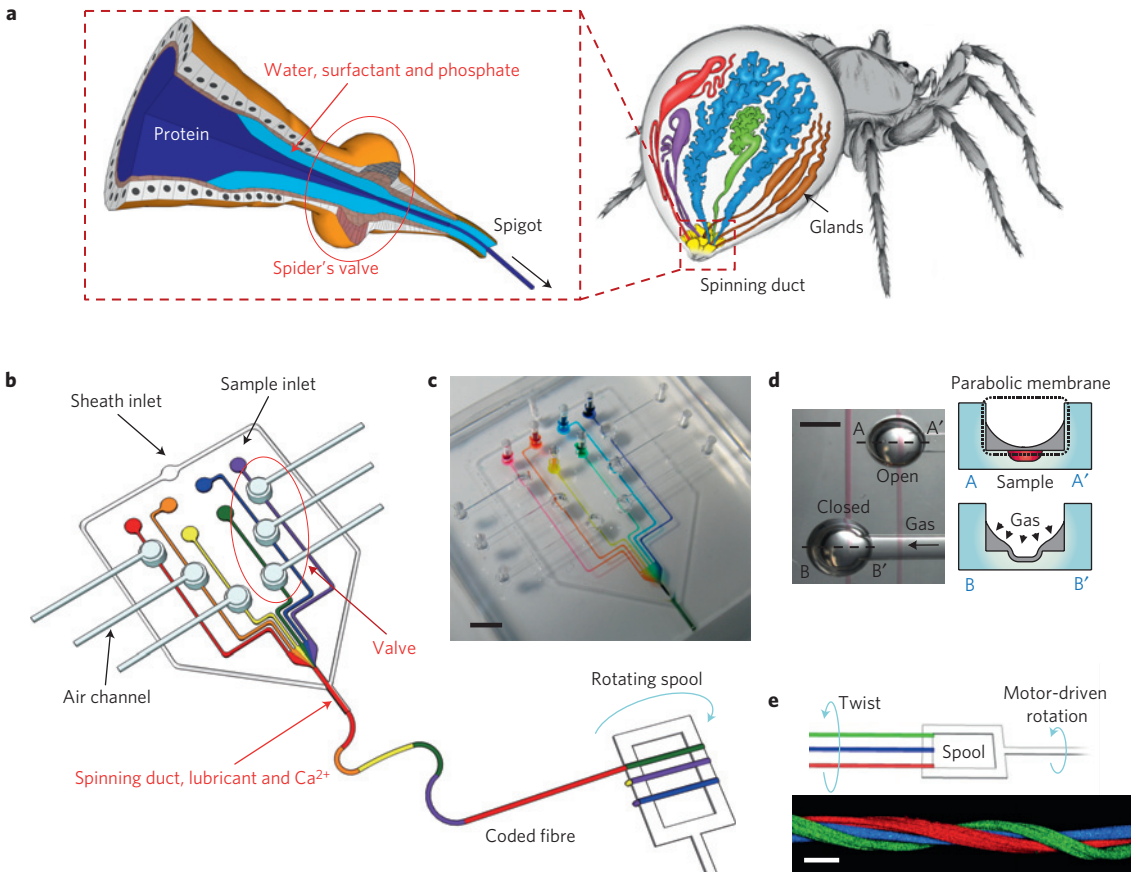

Figure 1 | Concept of coded microfibre production. a, Anatomy of the silk-spinning system of spiders. The silk gland produces several proteins, the spinning duct focuses and solidifies the protein solution and the valve controls the flow of the protein. **b**, Conceptual description of the process of generating coded fibres. The extruded fibres were continuously wound on the spool by a motorized system (Supplementary Movie S2). **c**, Photograph of the microfluidic spinning chip. **d**, Optical image of the 'open' and 'closed' states of the valve above the channel (left) and a cross-sectional schematic of the valve operation (right). **e**, Schematic of the process of twisting fibres using a motor system (top) and a fluorescence micrograph of a twisted fibre with red-, green- and blue-stained fibres (bottom, Supplementary Movie S6). Scale bars, 5 mm (**c**), 2 mm (**d**) and 500 μm (**e**).

of the pre-polymer PDMS with air (Fig. 1d; fabrication process and valve analysis is shown in Supplementary Figs S2 and S3). The end of the chip consists of cylindrical channels with various diameters to generate the coaxial flow (Supplementary Fig. S4). The sheath flow ($CaCl_2$) separates the alginate stream from the channel wall, shapes the focused sample flow (alginic acid) and induces subsequent sample gelation by chelation of the Ca^{2+} ions to form a solid alginate fibre[20]. The sheath fluid not only focuses the alginate flow, but also provides a lubricant layer during alginate gelation (Supplementary Information). In our experiments, alginate was used because it has been approved by the Food and Drug Administration for certain biomedical applications, although a range of other materials (for example, polyethylene glycol and chitosan) can also be used[8,21,22]. To control the alignment of the extruded fibres, they were wound around a small rotating spool. The relationship between the flow rates and the maximum winding velocity of the motor is shown in Supplementary Fig. S4d (see Methods for detail). Furthermore, by twisting the fibres with a spool, triple-helix fibres were generated, as shown in Fig. 1e.

The proposed platform was used to code a range of chemical compositions within the fibres. To code chemical compositions in a microfibre, the fluid volume of each inlet channel was independently controlled by a pneumatic valve. Figure 2a shows a control scheme for valve operation to fabricate microfibres that contained different materials coded into them either in a serial, parallel or mixed (that is, containing both serial and parallel coated regions) manner. Figure 2b shows a photograph of a fibre produced with both serial and parallel coding, and Fig. 2c shows a fluorescence micrograph of a serially coded fibre. As can be seen, the controlled opening of upstream valves yielded a microfibre coded with different coloured dyes along its length. With the present set-up the smallest length of the serial coding was ~800 μm, although this is expected to improve with more advanced valves (Fig. 2c, inset, and Supplementary Fig. S7). Such coding has many potential applications for biosensing, high-throughput screening and the spatiotemporal cell positioning of heterogeneous cells for tissue engineering. Recently, Janus fibres coded in parallel have been reported[14,23]. However, serial or mixed coding of materials using a microfluidic device has not been demonstrated previously. Figure 2d illustrates a fibre coded with different compositions in parallel across the fibre, indicating that functional microscale fibres in which diverse chemicals and cells are spatiotemporally coded may be readily produced. Although a fibre with three parallel regions across its diameter is illustrated, the number and dimensions of the parallel coded regions are highly controllable and can be easily tuned based on the complexity of the upstream fluidic design.

We also investigated the use of spatially controlled microfibres for recreating functional structures associated with biological systems. Recently, it has been reported that a spider's web captures dew through microstructures on the silk fibres[24]. In this process, tiny water droplets initially condense on the puffs on the silk fibres, causing the puffs to shrink as water condenses to form periodic

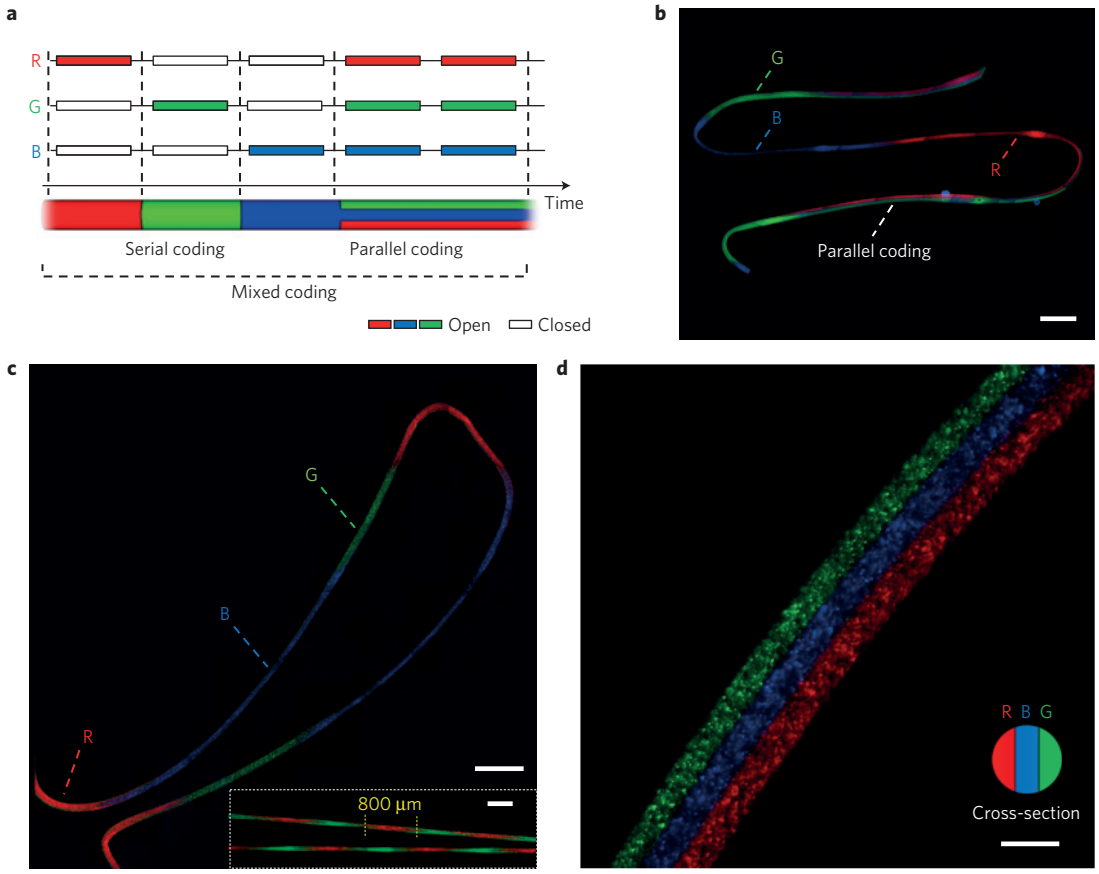

Figure 2 | Fabrication of spatially controlled microfibres with diverse chemical compositions. a, Schematic of the digital control steps for the microfluidic spinning chip for serial, parallel and mixed coding with various composite solutions (R, alginate solution with red fluorescent polystyrene beads; G, green; B, blue). **b**, Mixed coding (serial and parallel) of a fibre. **c**, Serially coded fibre (inset, serially coded fibre on the microscale) (Supplementary Movies S7 and S9). **d**, Parallel coding of fibres. Scale bars, 200 μm (**d**), 400 μm (**c**, inset) and 1 mm (**b**,**c**).

spindle-knots. The linking of spindle-knots and joints, as found in wet spider silk, contributes to directional water collection as a result of a surface-energy gradient and a difference in Laplace pressure. One of the advantages of the spinning chip developed here is that it can generate fibres with controllable topography and structure. The fibre diameter and length of spindle-knots can be modulated by the valve operation (Supplementary Fig. S5). Furthermore, the porosity of the resulting fibre can be controlled by changing the material that is coded along the fibre. As shown in Fig. 3a, we introduced two alternating fluid streams to generate continuous fibres with evenly spaced nanoporous spindle-knots. To construct a porous spindle-knot, we injected an alginate solution containing salt (0.5% w/w) at a high flow rate into one of the sample channels. It is noteworthy that the length of the spindle-knot could be controlled by altering the time that the valve was kept open.

We generated nanoporous structures in the spindle-knot by salt dissolution in the fibres (Fig. 3b). As illustrated in Fig. 3c, after leaching of salt, nanoporous structures were generated that had a higher surface energy than joint regions, which attracted water. At the same time, the tapered shape of the spindle-knot generated a difference in Laplace pressure, which provided a driving force for water movement. Figure 3d shows a photograph of an artificial fibre consisting of nanoporous spindle-knots and joints that closely resembles spider silk. To investigate the ability of the engineered fibres to mimic the water-collecting behaviour of spider silk, drops of water were added on the fibre. As expected, the water droplets self-collected at the spindle-knots, forming large droplets (Fig. 3e). Interestingly, the water-collecting capabilities of the fibres depended on the length of the spindle-knot. Figure 3f plots the volume of water droplets at the spindle-knot as a function of the length of the spindle-knot. The water droplet volume correlated linearly to the length of the spindle-knot ($r^2 = 0.97$). Such microfluidic coding of a heterogeneous structure may be useful for topics ranging from the basic understanding of the physiology of fibre spinning mechanisms in various organisms to practical applications involving water collection and purification.

In nature, tubuliform silk fibres, which are used to encapsulate eggs, have small grooves on their surfaces[25]. We fabricated artificial tubuliform fibres coded with grooves on the surface using a grooved round channel (Fig. 3g and Supplementary Fig. S6). As can be seen in Fig. 3h, grooved fibres could be fabricated in a highly uniform manner. Furthermore, the number and size of grooves can be tuned by changing the shape of the channel and flow rate. To assess the use of microgrooved fibres in tissue engineering applications, rat embryonic neurons (from embryos of pregnant Sprague–Dawley rats at 16 days of gestation) were placed on smooth and grooved fibres and analysed for their resulting cell alignment after 5 days. As shown in Fig. 3i, neurons extended neurites along the length of both smooth and grooved fibres; however, these extensions were significantly more aligned and controlled along the ridges of the nanogrooved fibres (see Methods for details). Such controlled alignment is of great importance in directing the extension of axons and controlling their subsequent connection with other cells, and has important implications in tissue regeneration after spinal cord or peripheral nerve injury.

More complex coding of morphology and composition in the fibre was also achieved. A slight modification of the material and flow control scheme enabled diverse morphologies and varying

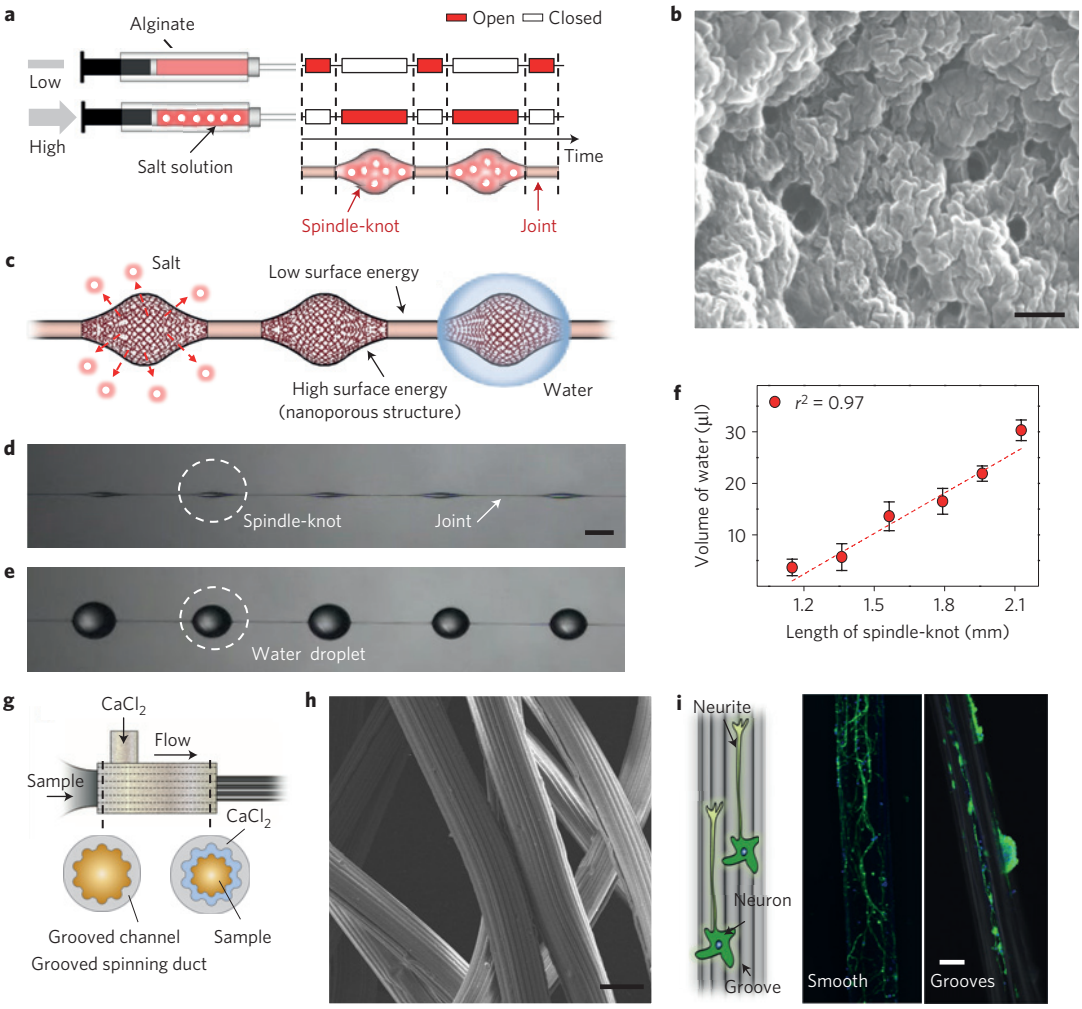

Figure 3 | Structural coding of fibres. a, Schematic of a digital control scheme for generating artificial spindle-knots and joints by means of topography modulation and nanoporous structure coding (Supplementary Movie S3). **b**, SEM image of a magnified spindle-knot where the rough and porous surface is apparent. **c**, Schematic of a fibre with a different surface energy and water-collection mechanism. **d**, Artificially spun fibres with spindle-knots and joints. **e**, Aggregation of water droplets at the artificial spindle-knots. **f**, Volume of water as a function of spindle-knot length. Data are expressed as mean ± s.d. ($n \geq 10$). **g**, Schematic of groove coding on the fibre surface using a grooved round channel. **h**, Grooved fibres fabricated using the spinning chip. **i**, Schematic of neuron alignment on a grooved fibre (left) and fluorescence micrograph of neurons on a fibre without grooves (middle) and on a grooved fibre (right) (green, neurofilament; blue, nucleus). Scale bars, 200 nm (**b**), 1 mm (**d**), 20 μm (**h**) and 50 μm (**i**).

compositions to be coded along the length of the fibre. As shown in the control scheme of Fig. 4a, the periodic modulation of fibre diameter and the coding of varying composition were carried out simultaneously. Figure 4b,c shows fluorescence micrographs of the fibres, indicating that fibres with spatiotemporal variations in morphology and chemical composition could be produced using a single microfluidic platform and digital control scheme. The diameter of the fibre could be periodically tapered by controlling valve operation. Figure 4d shows the control scheme to produce tapered fibres. By periodically opening one and two valves, tapered fibres were produced (Fig. 4e) and multiple 3 μm grooves were engraved on the fibre surface, as shown in Fig. 4f. In addition to aqueous gels, gas could also be coded along the fibres. This was achieved by injecting gas and detergent into the alginate solution channel to fabricate microfibres that contained gas bubbles. By operating the valve at controlled intervals, gas could be distributed either periodically or uniformly throughout the fibres (Fig. 4g). Figure 4h shows an image of a gas-coded fibre in which the period and the size of the gas bubbles were controlled by changing the injecting gas pressure. Figure 4i shows an scanning electron microscopy (SEM) image of a gas-coded fibre. Although gels have a relatively high porosity (the diffusion coefficient of oxygen in alginate is 3.66×10^{-10} m^2 s^{-1}; ref. 26), after implantation the presence of a hypoxic microenvironment results in cell death before the formation of blood vessels. Thus, gas-coded fibres could be of potential benefit for providing a temporary source of oxygen to encapsulated cells.

We further demonstrated the feasibility of fibres for tissue engineering by generating three-dimensional structures with controlled cellular organization. As shown in Fig. 5a, we encapsulated primary rat hepatocytes and L929 fibroblasts along the length of the fibre either individually or as co-cultures (see Methods for details). Figure 5a, inset, shows an optical image of a fibre consisting of three regions and the magnified images of each region. In the co-cultured region, the fibroblasts and hepatocytes were coded in parallel (Fig. 5b and Supplementary Fig. S8). Figure 5c illustrates that most of the cells remained viable after being cultured for 1 and 3 days either individually or in co-culture. Interestingly, the fraction of viable cells in hepatocyte-only cultures decreased throughout the 5-day experiment, whereas the cells in co-cultures better maintained their viability. This result indicates that the spatiotemporal control of co-culturing

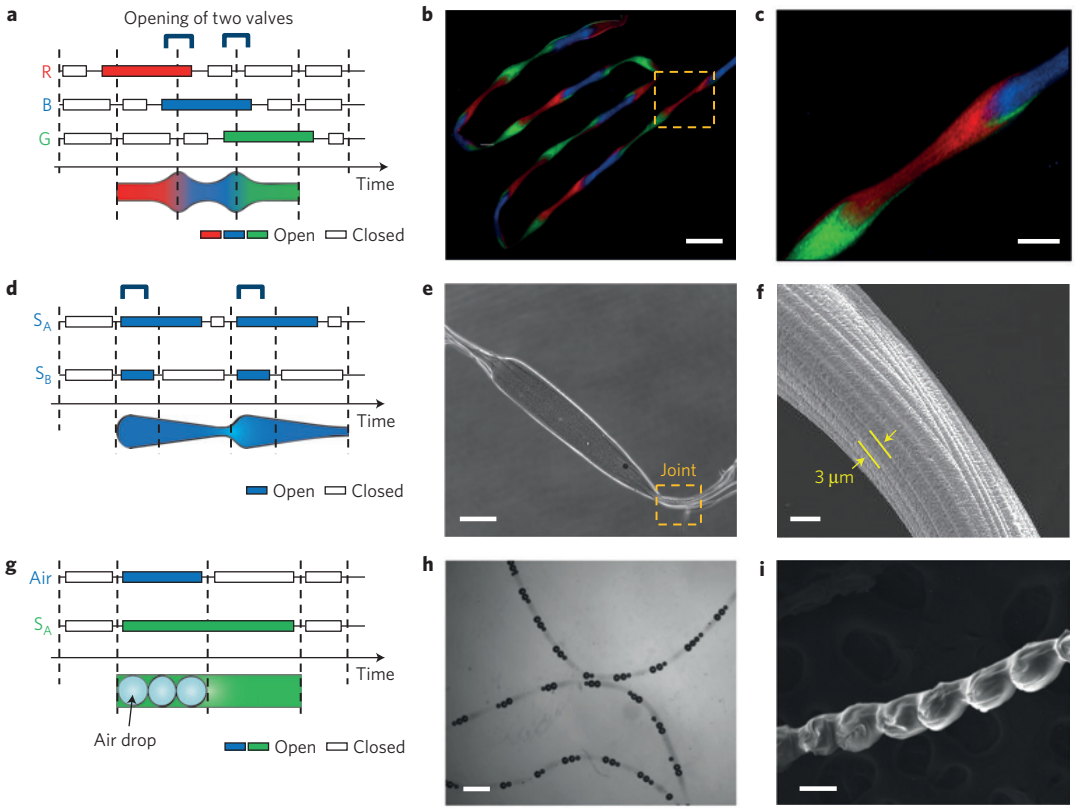

Figure 4 | Hybrid coding of fibres. a, Schematic of a digital control scheme to generate a fibre with spatiotemporal variations in morphology and chemical composition (R, alginate solution with red fluorescent polystyrene beads; G, green; B, blue). **b**,**c**, Fluorescence micrograph (**b**) and magnification (**c**; showing the area outlined in orange in **b**) of an embossed fibre coded serially with polystyrene beads (Supplementary Movie S8). **d**, Schematic of a digital control scheme for generating tapered fibres (S_A, alginate solution A; S_B, alginate solution B). **e**, Micrograph image of a tapered fibre (Supplementary Movie S4). **f**, The grooved surface of a tapered fibre (orange outline in **e**). **g**, Schematic of a digital control scheme for coding gas bubbles in a fibre. **h**,**i**, Light microscopy (**h**) and SEM (**i**) images of a fibre coded with air bubbles (Supplementary Movie S5). Scale bars, 5 μm (**f**), 50 μm (**i**), 1 mm (**b**,**h**) and 300 μm (**c**,**e**).

within the scaffold is of potential benefit in tissue-engineering applications and cell-biology studies. To further demonstrate the use of chemical coding in the study of cell behaviour, we coded a neutrophil chemoattractant, formyl-Met-Leu-Phe (fMLP, concentration: 10 μM), periodically in a fibre (Fig. 5d) and placed the fibre inside a culture containing neutrophils (see Methods for detail). The presence of fMLP in neutrophil cultures induced immediate cell polarization and subsequent migration towards the fMLP source. Figure 5e shows fluorescence micrographs at the boundary between two segments of the fibre after 30 min, 3 and 6 h of exposure. As can be seen, the neutrophils migrated towards the fMLP-coded region, as tracked by the arrows. This behaviour is quantified in Fig. 5f. Thus, the coded fibres may be used to modulate the migration of surrounding cells in a spatially controllable manner.

We have presented a spinning method that uses a microfluidic chip combined with a digital fluid controller for the versatile tuning of chemical and morphological properties on the micrometre scale. The coding of diverse materials on the microscale may offer new opportunities to generate a range of useful functions in materials. Nature also uses spatial patterning of existing materials to generate new functionality. The proposed method can be used to fabricate many other materials in a spatially regulated manner to generate functional fibres of benefit for a variety of applications including tissue engineering and drug delivery. Furthermore, this microengineering approach may encourage innovation in a wide range of application areas in the future, such as water purification, neuron-cell alignment for nerve regeneration and development of new functional textiles.

Methods

Valve control system. To operate the small pneumatic valves, compression and vacuum pumps were employed. Supplementary Fig. S1 illustrates the set-up for valve control. Continuous air pressure (around 200 kpa) or vacuum was supplied, and the 'on–off' switching of air flow was controlled using solenoid valves. The 'open' and 'closed' operations of the solenoid valve were controlled using a program written in Lab View (NI Lab View 8.6.1, National Instruments). Communication between the Lab View routine and the solenoid (ST2001-15DN, DKC) proceeded through a data acquisition board (NI DAQ-PAD 6015/6016, National Instruments).

Flow focusing and winding system. The end of the chip consisted of cylindrical channels with various diameters to generate the coaxial flow, and the sheath flow plays a key role to focus the sample flow stream (Supplementary Fig. S4a). Supplementary Fig. S4b shows an SEM image of a coaxial channel. Supplementary Fig. S4c illustrates the winding system for extruded fibre and the wound fibres on the spool (Supplementary Fig. S4c, inset). By altering the motor speed, the fibres were successfully wound around the rotating rectangular spool (acryl spool: width 15 mm × 20 mm, height 2 mm) without breaking. A d.c. geared micromotor (PGM30-2838E, Motor Bank, Korea) was used in the winding system and the range of d.c. used was from 6 V to 12 V. The relationship between the flow rates and the maximum winding velocity of the motor is illustrated in Supplementary Fig. S4d.

Co-culture of primary rat hepatocytes and fibroblasts in the fibres. Hepatocytes and fibroblasts were co-cultured in the fibre using primary rat hepatocytes and L929 (mouse fibroblast cell line) cells. L929 cells were cultured in Dulbecco's modified Eagle's medium (DMEM, Gibco) supplemented with 10% fetal bovine serum, 100 μg streptomycin and 100 unit ml^{-1} of penicillin. Cells were embedded in the fibre using a spinning chip with three sample channels. First, we dispersed hepatocytes and L929 cells in a 1 wt% alginate solution mixed with a 2 wt% chitosan solution and a 1 wt% alginate solution at a concentration of 5×10^6 cells ml^{-1}. The solution with hepatocyte cells was introduced through the middle channel at an average flow rate of ~10 μl min^{-1}. The solution with the L929 cells was introduced through the side channels at the same flow rate. Ten minutes after fibre generation, the fibre was moved to the cell-culture well containing primary

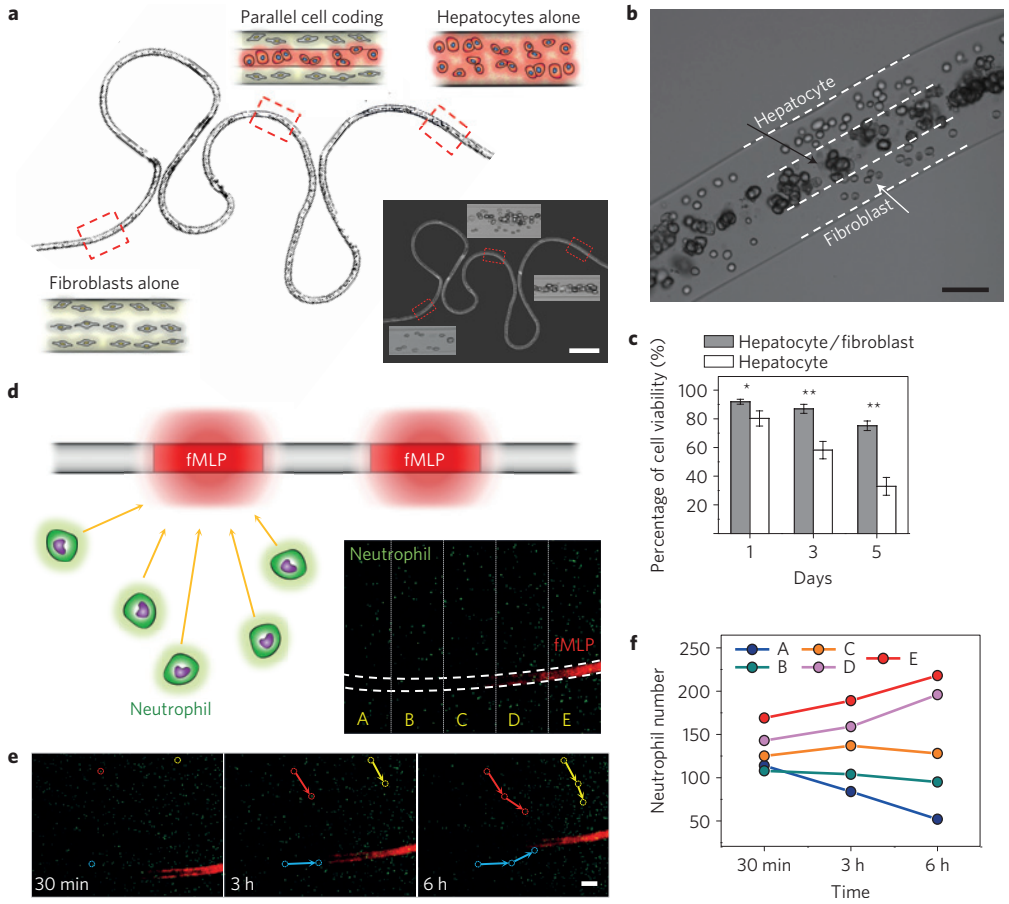

Figure 5 | Spatially coded microfibres for three-dimensional tissue culture. a, Schematic of a periodically coded fibre with either primary rat hepatocytes, fibroblasts (L929) or a mixture of hepatocytes and fibroblasts. Insets, optical image of cells in a fibre (bottom right) and micrographs of embedded cells in a fibre (fibroblasts alone, bottom left; mixture of fibroblasts and hepatocytes, top left; hepatocytes alone, top right). **b**, Magnified image of a co-culture region that consists of multiple parallel layers of either hepatocytes or fibroblasts. **c**, Hepatocyte and L929 cell viability in two different fibres during a 5-day experiment. Data are expressed as mean ± s.d. ($n \geq 10$; *, $P < 0.005$; **, $P < 0.0005$; two-tailed t-test). **d**, Schematic of a fibre periodically coded with fMLP, which mediates neutrophil migration; inset, fluorescence micrograph of the boundary between two segments of a fibre (green, neutrophil; red, fMLP). **e**, Time-lapse images at the boundary between two segments of a fibre at 30 min, 3 h and 6 h (the arrows represent time-lapse traces of 3 cells). **f**, The cell number of each region (A to E) over time. Scale bars, 1,000 μm (**a**) and 100 μm (**b**,**e**).

hepatocyte culture medium. The cells were incubated in an incubator over the next 5 days. Cell viability was measured using a live/dead assay (L3224, Invitrogen) each day, following the protocol mentioned above.

Neural-cell culture on fibres. Grooved fibres and non-grooved fibres were prepared as previously described. After winding fibres on a spool, the fibres were dehydrated using ethanol ranging from 50% to 100%, and then dried in an oven at 80 °C overnight. Dried fibres were coated with poly-L-ornithine hydrobromide (0.1% in deionized water, Sigma) and laminin (5 ug ml^{-1} in deionized water, Roche) for 10 min and 1 h respectively. Neuron cells isolated from rat embryos were diluted to 1×10^6 cells ml^{-1} and then seeded on fibres. Cell-culture medium was changed every 2 days. After 5 days, the neuronal cells were immunostained to identify neural alignments on fibres. Fibres with cells were fixed in 4% paraformaldehyde for 4 h at 4 °C and permeabilized by 0.1% Triton X-100 for 20 min at room temperature. Next, fibres with cells were blocked with 3% BSA for 30 min and incubated with primary antibody at 4 °C overnight. Primary anti-GFAP antibodies (StemCell Technologies), which were specific for neurofilament, were used to visualize the location of the neuron. After incubating samples overnight, fibres with cells were washed with 0.1% BSA for 5 min. Alexa Fluor 488 goat anti-rabbit secondary antibody (1:500 dilution, Invitrogen) was applied for 1.5 h at room temperature and washed with 0.1% BSA. Fluorescence micrographs were acquired using confocal microscopy (Olympus) after counterstaining with 4,6-diamidino-2-phenylindole dihydrochloride (DAPI, Invitrogen). All reagents were diluted with pure neurobasal medium to prevent the alginate fibre from dissolving.

Neutrophil migration. An alginate solution of 1% concentration was mixed with 10 μM fMLP (Invitrogen), 0.1% dimethylsulphoxide and 0.05% fluorescent nanobeads. The mixed solution was then periodically coded into fibre. After winding the coded fibre on a spool, it was preserved at room temperature (dried fibre is stored at 4 °C). Fully differentiated neutrophils were diluted to a density of 5×10^5 cells ml^{-1} in culture medium and seeded on a culture chip. After cell inoculation, fMLP-coded fibres were placed on a culture channel, and covered by a glass slide. To observe neutrophil migration, time-lapse images were acquired using a fluorescence microscope (AxioVision 4) for a time duration of 8 h (Supplementary Movie S10).

Received 3 February 2011; accepted 1 August 2011; published online 4 September 2011

References

1. Daher, R. J., Chahine, N. O., Greenberg, A. S., Sgaglione, N. A. & Grande, D. A. New methods to diagnose and treat cartilage degeneration. *Nature Rev. Rheumatol.* **5,** 599–607 (2009).
2. Silva, G. A. *et al.* Selective differentiation of neural progenitor cells by high-epitope density nanofibers. *Science* **303,** 1352–1355 (2004).
3. Moutos, F. T., Freed, L. E. & Guilak, F. A biomimetic three-dimensional woven composite scaffold for functional tissue engineering of cartilage. *Nature Mater.* **6,** 162–167 (2007).
4. Shi, J. J., Votruba, A. R., Farokhzad, O. C. & Langer, R. Nanotechnology in drug delivery and tissue engineering: From discovery to applications. *Nano Lett.* **10,** 3223–3230 (2010).
5. Greiner, A. & Wendorff, J. H. Electrospinning: A fascinating method for the preparation of ultrathin fibres. *Angew. Chem. Int. Ed.* **46,** 5670–5703 (2007).
6. Sill, T. J. & von Recum, H. A. Electro spinning: Applications in drug delivery and tissue engineering. *Biomaterials* **29,** 1989–2006 (2008).

7. Hu, M. *et al.* Hydrodynamic spinning of hydrogel fibers. *Biomaterials* **31,** 863–869 (2010).
8. Rammensee, S., Slotta, U., Scheibel, T. & Bausch, A. R. Assembly mechanism of recombinant spider silk proteins. *Proc. Natl Acad. Sci. USA* **105,** 6590–6595 (2008).
9. Pregibon, D. C., Toner, M. & Doyle, P. S. Multifunctional encoded particles for high-throughput biomolecule analysis. *Science* **315,** 1393–1396 (2007).
10. Xu, Q. B. *et al.* Preparation of monodisperse biodegradable polymer microparticles using a microfluidic flow-focusing device for controlled drug delivery. *Small* **5,** 1575–1581 (2009).
11. Breslauer, D. N., Muller, S. J. & Lee, L. P. Generation of monodisperse silk microspheres prepared with microfluidics. *Biomacromolecules* **11,** 643–647 (2010).
12. Chung, S. E., Park, W., Shin, S., Lee, S. A. & Kwon, S. Guided and fluidic self-assembly of microstructures using railed microfluidic channels. *Nature Mater.* **7,** 581–587 (2008).
13. Mandal, S., Bhaskar, S. & Lahann, J. Micropatterned fiber scaffolds for spatially controlled cell adhesion. *Macromol. Rapid Commun.* **30,** 1638–1644 (2009).
14. Bhaskar, S., Hitt, J., Chang, S. W. L. & Lahann, J. Multicompartmental microcylinders. *Angew. Chem. Int. Ed.* **48,** 4589–4593 (2009).
15. Jeong, W. *et al.* Hydrodynamic microfabrication via 'on the fly' photopolymerization of microscale fibers and tubes. *Lab Chip* **4,** 576–580 (2004).
16. Breslauer, D. N., Lee, L. P. & Muller, S. J. Simulation of flow in the silk gland. *Biomacromolecules* **10,** 49–57 (2009).
17. Kang, E., Shin, S. J., Lee, K. H. & Lee, S. H. Novel PDMS cylindrical channels that generate coaxial flow, and application to fabrication of microfibers and particles. *Lab Chip* **10,** 1856–1861 (2010).
18. Vollrath, F. Biology of spider silk. *Int. J. Biol. Macromol.* **24,** 81–88 (1999).
19. Vollrath, F. & Knight, D. P. Liquid crystalline spinning of spider silk. *Nature* **410,** 541–548 (2001).
20. Shin, S. *et al.* "On the fly" continuous generation of alginate fibers using a microfluidic device. *Langmuir* **23,** 9104–9108 (2007).
21. Kang, E., Lee, D. H., Kim, C. B., Yoo, S. J. & Lee, S. H. A hemispherical microfluidic channel for the trapping and passive dissipation of microbubbles. *J. Micromech. Microeng.* **20,** 045009 (2010).
22. Hwang, C. M., Khademhosseini, A., Park, Y., Sun, K. & Lee, S. H. Microfluidic chip-based fabrication of PLGA microfiber scaffolds for tissue engineering. *Langmuir* **24,** 6845–6851 (2008).
23. Jung, J. H., Choi, C. H., Chung, S., Chung, Y. M. & Lee, C. S. Microfluidic synthesis of a cell adhesive Janus polyurethane microfiber. *Lab Chip* **9,** 2596–2602 (2009).
24. Zheng, Y. M. *et al.* Directional water collection on wetted spider silk. *Nature* **463,** 640–643 (2010).
25. Blackledge, T. A. & Hayashi, C. Y. Silken toolkits: Biomechanics of silk fibers spun by the orb web spider *Argiope argentata* (Fabricius 1775). *J. Exp. Biol.* **209,** 2452–2461 (2006).
26. Renneberg, R., Sonomoto, K., Katoh, S. & Tanaka, A. Oxygen diffusivity of synthetic gels derived from prepolymers. *Appl. Microbiol. Biot.* **28,** 1–7 (1988).

Acknowledgements

This study was supported by a grant from the NRL (National Research Laboratory) programme, the Korea Science and Engineering Foundation (KOSEF), Republic of Korea (No. 20110020455), basic Science Research Program through the National Research Foundation of Korea (NRF) funded by the Ministry of Education, Science and Technology (No. R11-2008-044-02002-0) and the Korea Research and Engineering Foundation (KOSEF) funded by the Korea government (KRF; No. KRF-2008-220-D00133).

Author contributions

E.K. designed and carried out the experiments and prepared most of the data; G.S.J. carried out an analytical study of the valve system and assisted with the experiments; Y.Y.C. carried out the cell-based evaluation; K.H.L. optimized the material and developed the flow analysis; A.K. consulted on the manuscript and contributed in writing the paper; S-H.L. proposed the idea, managed the research process and wrote the paper.

Additional information

The authors declare no competing financial interests. Supplementary information accompanies this paper on www.nature.com/naturematerials. Reprints and permissions information is available online at http://www.nature.com/reprints. Correspondence and requests for materials should be addressed to S-H.L.